Surface-state induced inter-electrode isolation of *n*-on-*p* devices in mixed-field and γ-irradiation environments

T. Peltola [1], T. Abdilov [1], N. Akchurin [1], M. Harris [1], Y. Kazhykarim [1], V. Kuryatkov [2]

[1] Department of Physics and Astronomy, Advanced Particle Detector Laboratory, Texas Tech University, 1200 Memorial Circle, Lubbock, Texas, U.S.A.

[2] Nanotech Center, Texas Tech University, 902 Boston Ave, Lubbock, Texas, U.S.A.

1. Introduction – Inter-strip resistance of hadron/mixed-field vs X-ray irradiated sensors

- ❑ ***N*-on-*p* Si-sensors:** Advantages in extreme radiation environments in terms of radiation hardness over the traditional *p*-on-*n* sensors include:
  - Electron collection instead of holes
  - Overlapping maxima of weighting and electric fields at the charge-collecting electrodes
  - ○ **Drawback:** Radiation-induced accumulation of positive net oxide charges (N_{ox}) under the Si/SiO$_2$-interface that at high densities can compromise the position resolution by creating a conduction channel between the electrodes
- ❑ **Radiation-induced surface damage:**
  - **Ionizing radiation:** X-rays/γs/charged particles (p, *e*,…) → accumulation of fixed oxide charge (N_f) and interface trap (or surface states N_{it}) densities
  - **Displacement damage:** Neutral/charged particles (n, p,…) → accumulation of N_{it}
- ❑ **Neutron radiation environment:** Mixed field of neutrons with background γs (n/γ)
- ❑ **Previous studies:**
  - ***N*-on-*p* sensors with *p*-stop isolation implant up to ~700 kGy:** Dose (*D*) dependence of inter-strip resistance (R_{int}) for X-rays disappears for n/γ+X-ray irradiated [1]
  - ***N*-on-*p* without *p*-stop:** Significantly higher R_{int} for ~3-6 kGy n/γ- and ~870 kGy p-irradiated than for 3 kGy X-rays [2]

→ different introduction rates of N_f and/or N_{it} at Si/SiO$_2$-interface between irradiation types?

2. Observations on oxide-charge and surface-state accumulation with dose: Measured and TCAD-simulated MOS *CV*-characteristics: n/γ- vs γ-irradiated

- ❑ **Irradiation campaigns of MOS-capacitors [3]:**
  - **n/γs:** RINSC (Rhode Island) and MNRC reactors (UC Davis)
  - **γs(^{60}Co):** GIF (Sandia)

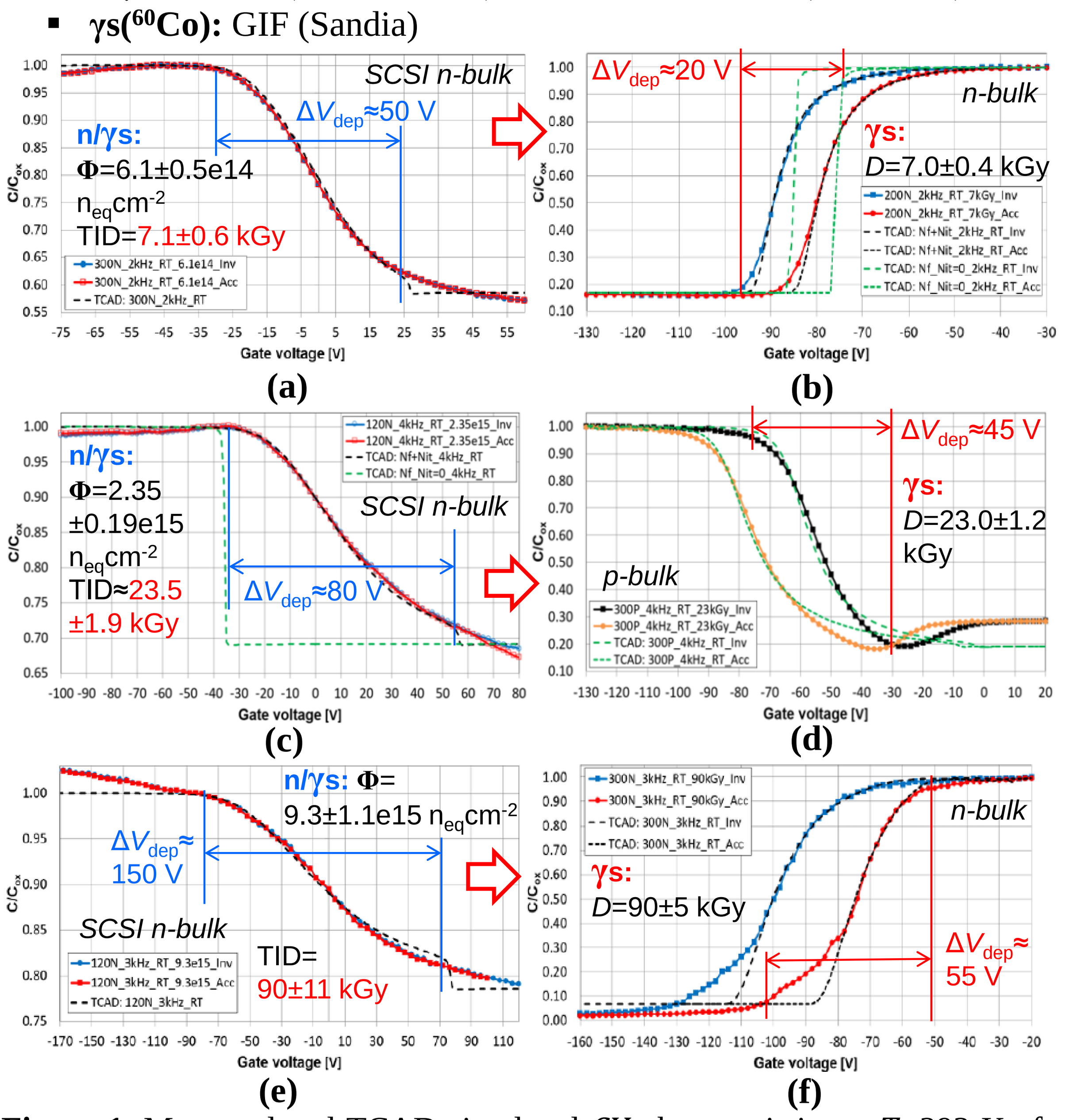

Figure 1. Measured and TCAD-simulated *CV*-characteristics at *T*=293 K after n/γ- or γ-irradiations for a (a) 300-μm-thick initial *n*-bulk (Space Charge Sign-Inverted (SCSI) to *p*-bulk) MOS-capacitor, (b) 200-μm-thick *n*-bulk MOS, (c) 120-μm-thick SCSI-*p*-bulk MOS, (d) 300-μm-thick *p*-bulk MOS, (e) 120-μm-thick SCSI-*p*-bulk MOS, and (f) 300-μm-thick *n*-bulk MOS. Measurements included *CV*-sweeps starting from both inversion (Inv.) and accumulation (Acc.) regions [3].

- ❑ ***γ*-irradiated MOS in Fig. 1:** Substantially shorter depletion region (ΔV_{dep}) compared to mixed-field irradiated
  - **Hysteresis between Inv./Acc. *CV*-sweeps:** Only observed in γ-irradiated MOSs
- ❑ **Measured *CV*-characteristics reproduced by TCAD in Fig. 1:** Requires introduction of both donor- and acceptor-type deep N_{it} at Si/SiO$_2$-interface (in addition to N_f) in Table 1
  - **Only N_f at the Si/SiO$_2$-interface in Figs. 1b, c (green dash):** Abrupt depletion region that does not reproduce the measured MOS *CV*-characteristics

Table 1. The simulation input parameters of radiation-induced N_{it}. $E_{a,V,C}$ are the activation energy, valence band and conduction band energies, respectively, while $\sigma_{e,h}$ are the electron and hole trapping cross sections, respectively [3].

N_{it} type	E_a [eV]	$\sigma_{e,h}$ [cm^2]	Density [cm^{-2}]
Deep donor ($N_{it,don}$)	E_V + 0.65	1e-15	see Fig. 2
Deep acceptor ($N_{it,acc}$)	E_C - 0.60	1e-15	see Fig. 2

TCAD=Technology Computer-Aided Design
MOS=Metal-Oxide-Semiconductor
TID=Total Ionizing Dose

- ❑ **Surface-state dynamics [4]:**

Equation 1: $Q_{ox} = eN_{ox} = e(N_f + aN_{it,don} - bN_{it,acc})$ [3,5]

→ ***a* & *b*:** fractions of fully occupied $N_{it,don/acc}$

- ❑ N_f: always fully occupied
- ❑ **Unoccupied $N_{it,don}$ & $N_{it,acc}$:** Q_{it} = 0
- ❑ **Fully occupied $N_{it,don}$:** Q_{it} = +*e*
- ❑ **Fully occupied $N_{it,acc}$:** Q_{it} = −*e*

- ❑ **n/γ- vs γ-irradiated in Fig. 2:**
  - $N_{it,\ don/acc}$: Substantially higher introduction rate for n/γ-irradiated → reflected by significantly larger ΔV_{dep} in Fig. 1

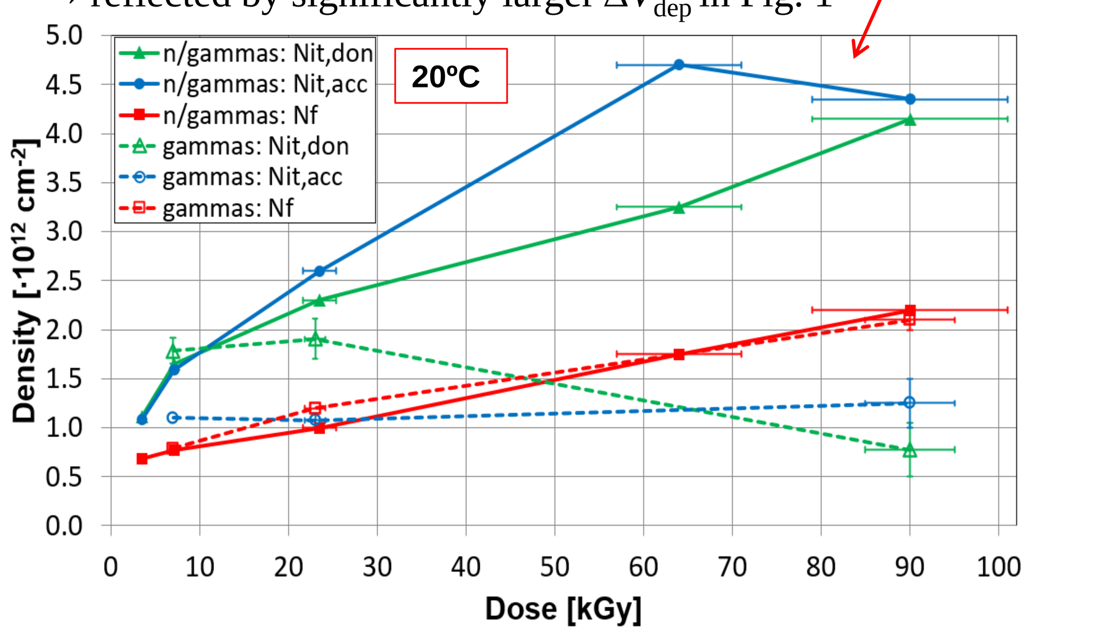

Figure 2: Simulated evolution of N_f and surface-state densities with dose for mixed-field and γ-irradiations. For clarity, mean values between densities extracted from *CV*-sweeps starting either from accumulation- or inversion-regions of the γ-irradiated MOSs in Figs. 1b, 1d & 1f are considered.

3. R_{int}-simulations

3.1 TCAD-modeled devices

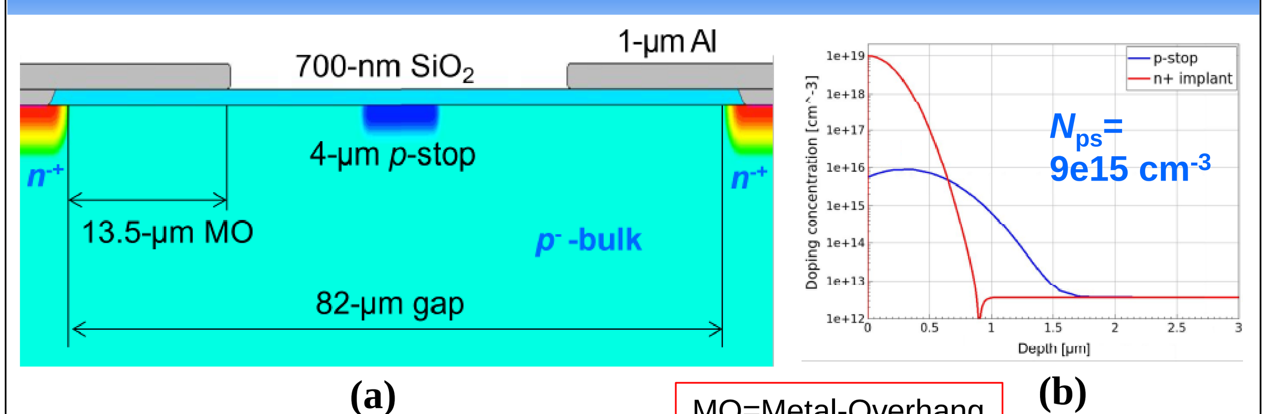

Figure 3: 2D-device structures implemented for the R_{int}-simulations. (a) Inter-pad region of a DC-coupled 300-μm-thick *n*-on-*p* pad-sensor with a ‘common’ *p*-stop. (b) Doping profiles of the n^+-implants and *p*-stop. (c) Inter-strip region of a strip-sensor with ‘individual’ *p*-stops. Doping profiles are identical to Fig. 3b, except for *p*-stop peak doping N_{ps}=1.5·10^{16} cm^{-3}.

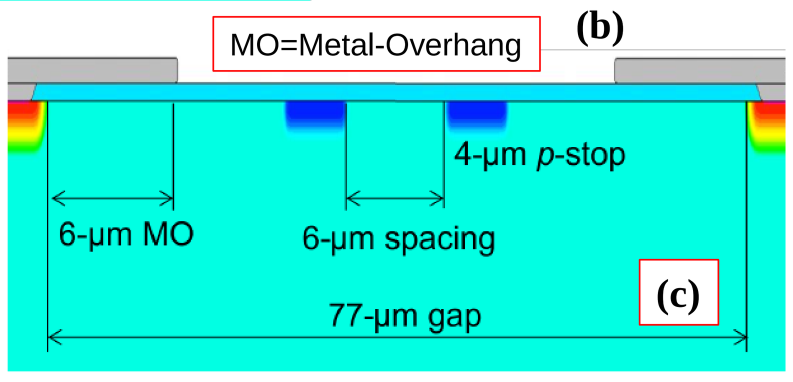

3.2 $R_{int}(V, D)$ with N_f/N_{it} -parameters as input: n/γ- vs γ-irradiated with and without *p*-stop

- ❑ **R_{int}-results:** Normalized to inter-electrode resistivity (ρ_{int}) → enables comparison with varied geometry devices

$$\rho_{int} = R_{int}\frac{A}{L} = R_{int}\frac{w \cdot d}{L}$$

w=strip length (=width)
d=strip-implant depth
L=gap length between strips

- ❑ **Limits for sufficient strip-solation:**

$\rho_{int,min}$(CMS HGCAL) ≈ 0.9 kΩ·cm ≈ preamplifier Z_{input} ·100

$\rho_{int,min}$(CMS Tracker) ≈ 2.0 MΩ·cm ≈ R_{bias}·100 [2]

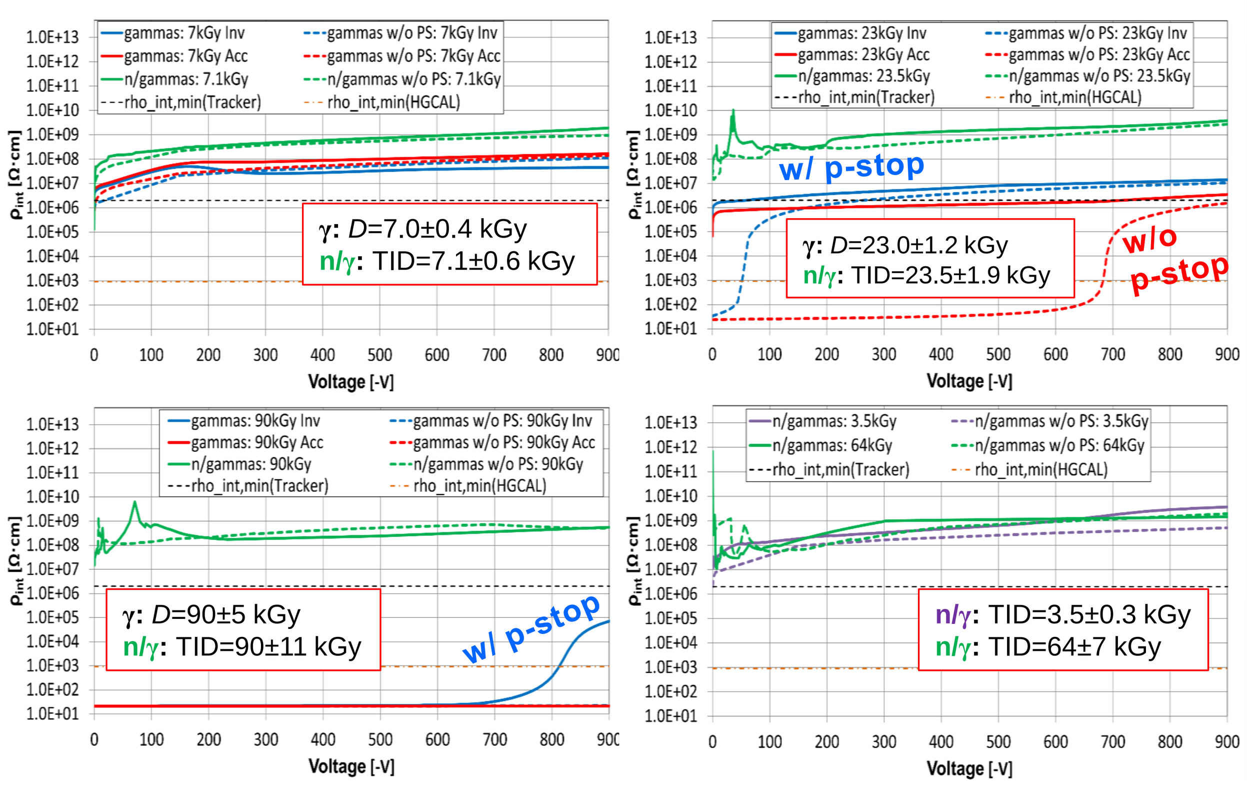

Figure 4: Simulated evolution of ρ_{int} with reverse bias voltage at *T*=253 K for γ- or mixed-field irradiated *n*-on-*p* sensors with and without *p*-stop implants (‘w/o PS’).

- ❑ **n/γ-irradiated in Fig. 4:** High ρ_{int} for all TIDs for full *V*-range
  - ***p*-stop:** Irrelevant for isolation → beneficial impact to ρ_{int} from high introduction rate of N_{it}
- ❑ **γ-irradiated in Fig. 4:** Low ρ_{int}/shorted at *D*>23 kGy → low introduction rate of N_{it} → no benefit to ρ_{int}
  - ***p*-stop with N_{ps}=9e15 cm^{-3}:** Significant benefit to ρ_{int} only at 23 kGy

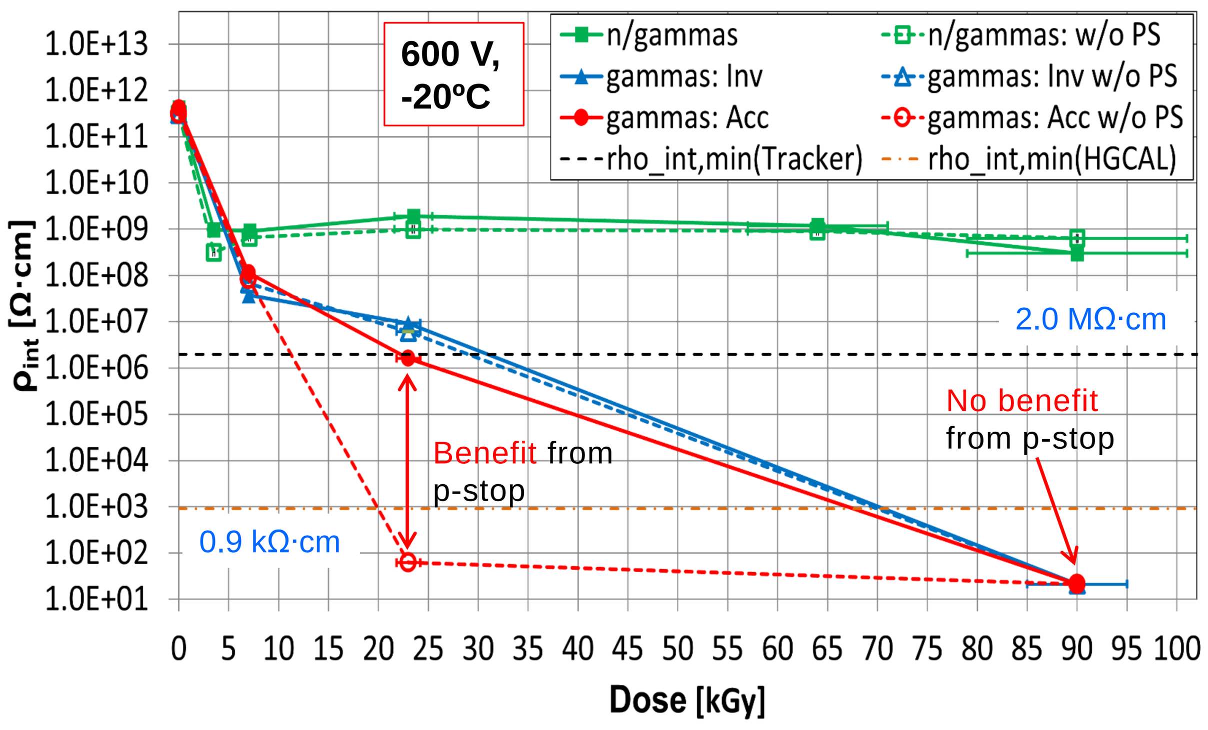

Figure 5: Simulated evolution of ρ_{int} with dose, extracted from Fig. 4 and from a pre-irradiated sensor simulation.

- ❑ **Mixed-field ρ_{int} in Fig. 5:** Essentially no TID and *p*-stop dependence → in line with experimental results for p, n/γ, p+n/γ-irradiated strip-sensors (with *p*-stop and *p*-spray) [6]
- ❑ **γ-irradiated ρ_{int} in Fig. 5:** Substantial dose dependence → difference between mixed field and γs in line with measured results for n/γ+X-rays vs X-rays in strip-sensors with *p*-stop [1]

3.3 γs/X-rays: Influence of p-stop doping on R_{int}

- ❑ **Varied N_{ps} in Fig. 6a:** ρ_{int} highly sensitive to the level of N_{ps} → comparative ρ_{int}-evaluations done with γs or X-rays between sensors can be convoluted by differences in N_{ps} (e.g. Tracker vs HGCAL sensors)

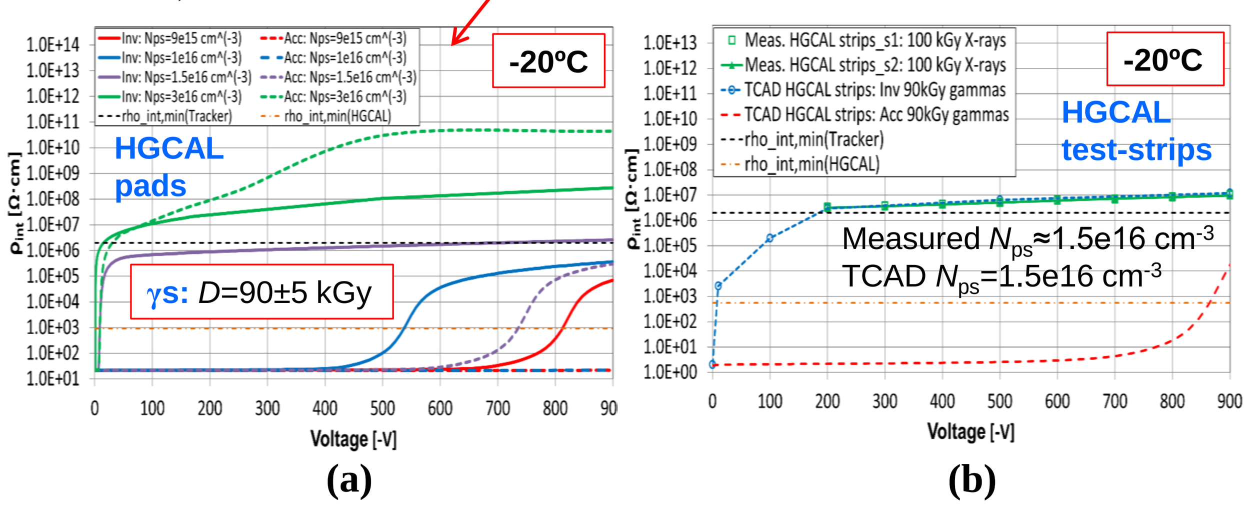

Figure 6: (a) Simulated influence of N_{ps} on ρ_{int} in a γ-irradiated sensor. (b) Comparison of measured and simulated ρ_{int} of irradiated HGCAL test-strips. The two measured test-strip samples were X-ray irradiated to *D*=100±10 kGy, while the simulation applied the surface-damage parameters for *D*=90±5 kGy from Table 1 and Fig. 2.

- ❑ **Measured vs TCAD in Fig. 6b:** Close agreement with N_f and N_{it} tuned for *CV*-sweep starting from negative voltages → *a*→1 in Eq. 1 models more accurately conditions at Si/SiO$_2$-interface between reverse-biased n^+-electrodes after γ- or X-ray irradiation

4. Conclusions

- ❑ **R_{int} -simulations of *n*-on-*p* pad-sensors:** Higher densities of deep $N_{it,acc/don}$ correlate with higher ρ_{int}
  - **ρ_{int} of γ-irradiated sensors:** Low introduction rates of deep $N_{it,acc/don}$ → high sensitivity to the presence and N_{ps} of *p*-stop
  - **ρ_{int} of n/γ-irradiated sensors:** High introduction rates of deep $N_{it,acc/don}$ → no sensitivity to the presence of *p*-stop → superior ρ_{int} performance to γ-irradiated for full dose range of about 100 kGy → *p*-stops not required to maintain high position resolution in mixed-field environment
  - **Neutron radiation:** Contribution to TID ~negligible → role in N_{it} introduction decisive
- ❑ **Reported saturation of accumulation of N_f and N_{it} at ~100–200 kGy [7,8,9]:** *N*-on-*p* sensors without *p*-stops → potentially feasible configuration for future HEP-experiments with radiation environments involving hadrons
  - **Similar number of lithography and ion-implantation steps to *p*-on-*n*:** Reduced processing cost of *n*-on-*p* sensors
  - **Sensor performance without *p*-stops:** Zero probability of discharges or avalanche effects due to excessive electric fields at *p*-stops

References

[1] V. Mariani, et al., NIM A 980 (2020) 164423.
[2] J.-O. Müller-Gosewisch, et al., 2021 JINST 16 P07004.
[3] N. Akchurin et al 2023 JINST 18 P08001.
[4] E.H. Nicollian and J.R. Brews, John Wiley & Sons (1982).
[5] Poehlsen et al., NIM A 700 (2013) 22-39.
[6] W. Adam, et al., JINST 12 (2017) P06018.
[7] J. Zhang, Ph.D. thesis, University of Hamburg, DESY-2013-00115 (2013).
[8] F. Moscatelli et al., IEEE Trans. Nucl. Sci. 64 (8) (2017) 2259–2267.
[9] F. Moscatelli, et al., JINST 12 (2017) P12010.